Original Research Article

The effects of drilling parameters on thrust force, temperature and hole quality of glass fiber reinforced polymer composites

Khurshid Malik[1], Faiz Ahmad[1] (ID), Woo Tze Keong[2] and Ebru Gunister[3] (ID)

Abstract
This paper presents an investigation of the drilling performance of glass fiber reinforced polymer (GFRP) composite based on the thrust force, temperature, and delamination factor (at entry and exit of the hole). High-speed steel (HSS), solid carbide (SC), and solid carbide Balinit® Helica coated (SCBH) twist tools were used for the drilling process. Other drilling parameters were high spindle speeds (12,000, 15,000, and 18,000 rpm), feed rate (300, 500, and 700 mm/min), and laminate thickness (3, 5, and 7 mm). ANOVA and response surface methodology were developed to examine the drilling process based on input and output parameters. Results showed that delamination was observed in the form of matrix debonding, uncut fibers, and fiber pull-out. The best drilling performance was achieved by the SC and SCBH tool at a low feed rate (300 rpm) and high speed (18,000 rpm), and high laminate thickness (7 mm).

Introduction

Glass fiber-reinforced polymer (GFRP) composites are prevalent in engineering applications because of their low cost and excellent properties compared to metals.[1,2] Therefore, they are commonly used in aerospace and marine industries.[3] For proper drilling operation, the composite parts must be joined during the final assembly, and around 70% of the machining processes involved drilling. Despite the development of various non-conventional drilling techniques, for instance, laser machining, water-jet machining, electrochemical, electro discharge, and electrochemical discharge to make the holes of composites, conventional mechanical drilling methods (such as milling, CNC drilling, and mechanical drilling) are still used as primary applications for fiber-reinforced polymer composites (FRPCs) due to financial benefits. Delamination is the main issue in FRPCs, which occurs due to the abrasive, hard, heterogeneous, and anisotropic fiber structure. Delamination influences the dimensional accuracy and surface finish of the hole, which causes the rejection of composite parts during the assembly stage.[4] There are many vital problems in FRPCs regarding drilling, such as fiber frying, spalling, chipping, fuzzing, fiber/matrix debonding, resin loss, uncut fiber, and fiber breaking compared to conventional materials.[5] Delamination influences the dimension accuracy and surface finishing of the hole, which causes the 60% parts rejection at the assembly stage.[6] The thrust force is a critical reason for delamination in GFRP composites.[7] Therefore, the thrust force must be kept low for a high-quality drilled hole. The lower thrust force could be found at a low feed rate and spindle speed.[8] Another crucial factor is the drilling-generated temperature that affects critical thrust force.[9] Feed rate and cutting speed have a crucial impact on delamination and thrust force.[10] Lower delamination (at entry and exit hole) in the GFRP composite could be achieved by drilling at a low feed rate and speed.[11] Hence, the optimization of these process parameters is required for good drilling

[1]Department of Mechanical Engineering, Faculty of Engineering, Universiti Teknologi PETRONAS, Perak, Malaysia
[2]Department of Mechanical Engineering, Politeknik Ungku Omar, Perak, Malaysia
[3]Department of Basic Sciences, Istanbul Galata University, Istanbul, Turkey

Corresponding author:
Faiz Ahmad, Department of Mechanical Engineering, Faculty of Engineering, Universiti Teknologi PETRONAS, Perak 32610, Malaysia.
Email: faizahmad@utp.edu.my

performance. High-speed drilling is an effective method to decline the drilling induce damage around the hole.[12,13] Tool diameter also plays a critical role in delamination.[14]

An investigation on the impact of various glass fiber/graphene/epoxy composite thicknesses on drilling performance was studied.[15] It was reported that lower thickness (2 mm) of composite had excellent performance for high-speed steel (HSS) drill at higher speed and lower feed rate. The effect of various drilling parameters such as feed rate and speed on delamination and tool wear for 6 mm thick of GFRP composite was examined.[16] It was found that the optimized condition was 951 rpm (speed) and 1 mm/min (feed rate) for the lowest delamination and tool wear. Another study on the drilling properties of 4 mm thick GFRP composite using various drill bits such as HSS, solid carbide, and tipped carbide.[17] It was reported that the HSS tool showed highest thrust force than other tools despite showing a higher delamination factor (DF). The temperature during the drilling operation of the GFRP composite having 8 mm thickness was examined and found that the feed rate has a greater influence on temperature than speed, and it rises with the feed rate at a higher speed.[18] The different laminate thicknesses (3, 6, 9, and 12 mm) of GFRPs using a carbide coated drill were investigated.[19] They reported that delamination augmented when the feed rate increased. However, a higher feed rate (150 mm/min) showed the opposite response. The thrust force with critical feed for GFRP composite drilling using a backup plate was also studied.[20] Tool angle and speed had a crucial impact on thrust force during drilling of GFRP composite.[21] The thrust force was higher (100 N-190 N) at low speed (600–1800 rpm) and a higher feed rate during GFRP composite drilling.[22] The heat and delamination during GFRP composite drilling were examined and found that high temperature was generated at a low feed rate for the HSS twist drill bit.[23] The poor drilling performance of carbon/nanocarbon/furfuryl resin hybrid composite using the Balinit® Helica coated carbide drill was also presented.[24] The thrust force, drilling temperature, and delamination of 20 mm thick of GFRP composite during the drilling operation were studied.[25] It was found that the temperature and thrust force were significantly influenced by speed and feed rate, respectively. Twist drill has better drilling performance than the candlestick tool in terms of lowering the thrust force, push-down, and peel-up delamination for GFRP composite.[26]

Although Balinit® Helica coated drill bit has been widely used in machining of the hard material such as alloy and metal compounds, there is no study in GFRP composite drilling using this tool, especially at a higher spindle speed. Moreover, most published studies focus on thrust force; they did not focus on the impact of generated temperature, which is inherent while performing the drilling. This paper is aimed to improve and analyze the drilling performance of GFRP composites. The main input variables are tool materials, speed, feed rate, and thickness. The drilling properties are measured based on output responses such as thrust force, temperature, DF at the entrance, and drilled hole exit. Analysis of variance (ANOVA) and response surface molding (RSM) is applied to process the drilling variables.

Materials and methodology

Materials and fabrication

E-glass was purchased from Castmech Technologies Sdn Bhd, Ipoh, Malaysia. It has a fiber diameter of 24 μm, 380 ± 40 g/m^2 of mass per unit area, 750 yarns per meter with 1.2 kg/m linear density, and fiber density of 2550 kg/m^3. Epicote 2820 was supplied by Wee Tee Tong Chemical Sdn. Bhd, Johore, Malaysia, and used as a matrix in the fabrication process. Epicote 2820 consists of two parts: part A, the epoxy, and part B, the hardener. The vacuum infusion molding (VIM) technique was used to fabricate the composites.[23] The E-glass and VIM fabrication process is given in Figure 1(a) and (b), respectively. Three GFRP
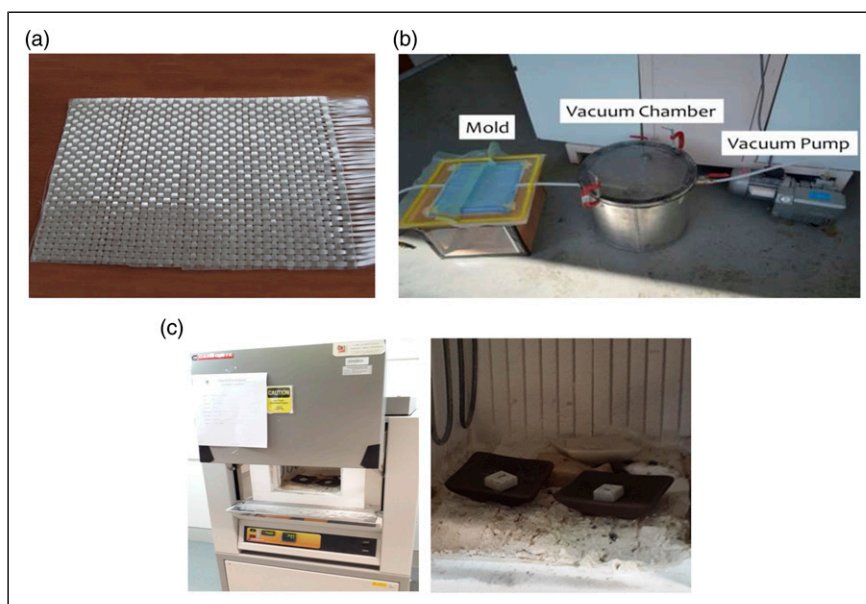

Figure 1. a) Twill woven glass fiber, b) VIM set up, and c) Carbolite CWF1300 used in resin burn off test.

plates were fabricated for each of three different thicknesses with a dimension of 35 cm x 35 cm and thickness of 3 mm, 5 mm, and 7 mm, respectively. The stacked of fiber clothes used in this study were 5 plies of woven glass fiber to produce 3 mm thick composite laminate test samples, 8 plies of woven glass fiber for the 5 mm thick composite laminate test samples, and 11 plies of woven glass fiber were used for the 7 mm thick composite laminate. It was ensured that the vacuum pressure used in the manufacturing process was set to 90 kPa and a motor power of 0.37 kW. The fabrication of the composites was done at room temperature. The impregnation process lasted 10, 12, and 15 min for the 3, 5, and 7 mm thick GFRP composites, respectively. Post-curing of the composites was done for 2 h at 90°C in the oven.

The composites' fiber volume fraction (FVF) was measured using the ASTM D 2584 burn-off test. The Carbolite Furnace CWF1300, which has a maximum working temperature of 1300°C, was used (Figure 1(c)). The specimens were heated in the furnace for around 30 min at around 550°C. For 30 min, the specimen burned evenly and moderately until the fiber remained and the burning stopped. The efficiency of this setup was checked by infusing without epoxy matrix to obtain the defect-free composite.

Equation (1) was used to calculate the FVF.[27] Where V, ρ, and W are FVF, density, and weight fractions of the specimen, respectively. Subscripts f, m, and p are fiber, matrix, and void contents.

$$V_f = \frac{\rho_m W_f}{\rho_f W_m + \rho_m W_f}, \ V_p = 1 - \left(V_f + V_m\right) \tag{1}$$

Although FVF was approximately 58% for all laminates, stable between 57.76% and 58.87%, which is well within the range for structural application (Table 1),[28] voids are due to the existence of air bubbles in the manufactured composites, which are referred to as void content. The void content was found to be less than 5%, which is considered a defect-free composite.[29,30] FVF increased while the void content dropped as the composite thickness increased. The vacuum bag's compression force increased throughout the vacuum infusion molding manufacture.[31] The fiberglass clothes stacking enabled a better flow of epoxy into the mold with a wider space between the vacuum bag and the molding platform with more plies of glass fiber clothes.[32] The vacuum bag compressed 11 plies of glass fiber more effectively than 5 plies of glass fiber garments under the same vacuum pressure of 90 kPa.

Drilling method

The drilling process was performed using the CNC milling machine, Mazak Variaxis 630, whose power and maximum speeds were 30 kW and 25,000 rpm, respectively. The drilling was carried out in dry condition. Three types of twist drill tools of 6 mm diameter, which are high-speed steel (HSS), solid carbide (SC), and solid carbide Balinit® Helica coated (SCBH), were selected to drill the hole in GFRP composite. All the physical properties of drill bits are the same such as 0.63 mm web thickness, 25 mm flute length, 118° point angle, 25° helix angle, and 143° chisel edge angle. However, the thermal conductivity (21, 84, and 75 W/m.K) of HSS, SC, and SCBH and the thermal expansion coefficient (9.7×10^{-6} K^{-1} and 5.5×10^{-6} K^{-1}) of HSS and SC drill bits were different due to material differences respectively. HSS tool is used for composite drilling because of low cost and easy availability, whereas solid carbide coated, and uncoated twist drill bits are more common in mass production at high speed.

The primary drilling factors are shown in Table 2.

Drilling process parameters such as spindle speed (12,000, 15,000, and 18,000 rpm), feed rate (300, 500, and 700 mm/min), and composite laminate thicknesses (3, 5, and 7 mm) were chosen based on published studies that found the most critical factors influencing the surface integrity of drilled holes on delamination, temperature, and thrust force during drilling.[10,19,21,33–40] These studies reported that faster material removal rates reduce the thrust force because of higher spindle speed. When employing a faster spindle speed, the heat generated during drilling has been indicated as a factor contributing to composite delamination; however, research on the heat generated during drilling is still restricted. When high-speed

Table 1. The fiber volume fraction of the fabricated GFRP composite.

GFRP thickness (mm)	Number of glass fiber plies	Fiber volume fraction (%)	Void content (%)
3	5	57.76	4.4
5	8	57.83	3.5
7	11	58.87	2.2

Table 2. Drilling process parameters and their levels.

Process parameters	Level 1	Level 2	Level 3
Speed (rpm)	12,000	15,000	18,000
Feed rate (mm/min)	300	500	700
Thick (mm)	3	5	7
Drill tool type	HSS	SC	SCBH

machining has been quickly adopted in various industries, it is critical to understand drilling-generated temperature in composite drilling. The feed rate has the most significant impact on the thrust force, which in turn has an impact on the delamination factor. For good quality of drilled hole, the increased downward force produced by using a higher feed rate must be adequately selected.[19,35,36,41–46] The feed rate is the most crucial delamination factor, followed by material thickness and drill bit diameter.[19,47–49] For each test case, an average of 10 holes were used to examine the drilling properties of the composites.

Measurement of drilling parameters

During drilling of GFRP composites, the thrust force was measured by a dynamometer (Kistler). As demonstrated in Figure 2(a), the dynamometer was equipped with three piezoelectric sensors covering the x, y, and z-axis. These sensors detect minute changes in force generated during the drilling experiment to a sensitivity of ±0.5 N. The signals detected by the sensors were then transmitted to the Kistler 9017b multichannel charge amplifier to be amplified and converted into a proportional voltage. These amplified voltages were then translated into thrust force versus time graph with a Dynoware equipped computer.

Two infrared thermometers (Edison EDI-312-4000K) were utilized to measure the drilling temperature; they placed 300 mm from the drill entering and exiting the GFRP composite test sample (as shown in Figure 2(b)). The temperature ranged between − 20°C to 537°C, at a response time of 0.5 s.

The DF is one of the vital variables used to examine the drilled hole quality. The specimens were investigated using a Mitutoyo 3D non-contact measuring system and QVPAK software to ensure no defects before the drilling process. The specimen with drilled holes was examined to capture images with four times magnification. The delaminated area is bulged because of damage that occurs near the drilled hole. The damaged part appears thick, and it creates differences in distance from the lens of the 3D non-contact measuring system to the drilled hole surface. The drilled hole's delaminated area is easier to detect by inverted using image processing software. Finally, the delaminated hole diameter is calculated using CAD software. As illustrated in Figure 2(c), DF was calculated by using equation (2),[39] where D_{max} and D_n are damaged hole' diameter and normal diameter of hole.

$$DF = \frac{D_{max}}{D_n} \qquad (2)$$

The design of experiments with RSM was conducted to examine the relationship between drilling input and output variables. ANOVA using the general linear model was run to analyze the most statistical parameters which impact the drilling performance (thrust force, temperature, and DF) of GFRP composites. The analysis was done to a significance level is 5% (confidence level of 95%). Finally, the optimized condition was determined based on tested parameters for GFRP composites. The Minitab 17 software was used to run the RSM.
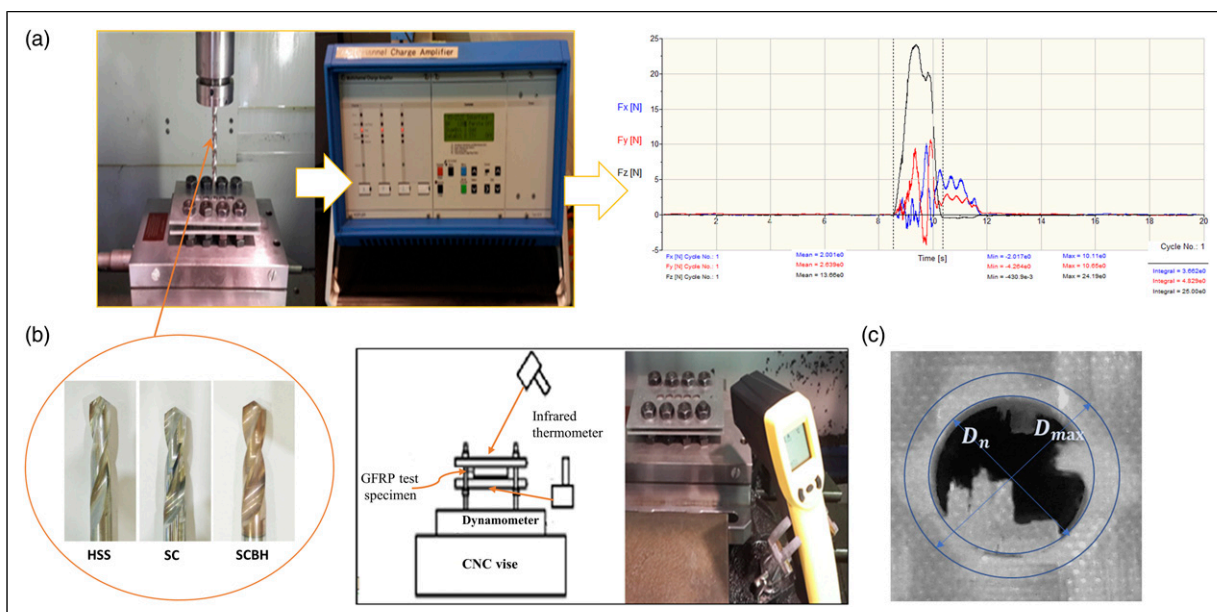

Figure 2. a) Thrust force measurement setup, b) temperature measurement setup, and c) DF measurement.

Table 3. Experimental conditions for drilling and the results for thrust force, temperature, and DF.

Test no.	Tool type	Speed	Feed	Thick	TF	Temp	DF (Entry)	DF (Exit)
1	HSS	12,000	300	3	10.61	29.30	1.36	1.44
2	HSS	12,000	300	5	12.92	50.35	1.33	1.52
3	HSS	12,000	300	7	16.36	64.13	1.26	1.46
4	HSS	12,000	500	3	14.01	26.89	1.32	1.52
5	HSS	12,000	500	5	15.50	37.11	1.31	1.49
6	HSS	12,000	500	7	16.34	46.39	1.29	1.45
7	HSS	12,000	700	3	16.04	28.86	1.29	1.49
8	HSS	12,000	700	5	19.03	29.63	1.36	1.57
9	HSS	12,000	700	7	22.47	48.93	1.33	1.48
10	HSS	15,000	300	3	8.47	28.27	1.29	1.41
11	HSS	15,000	300	5	13.42	42.56	1.28	1.40
12	HSS	15,000	300	7	15.96	76.65	1.29	1.46
13	HSS	15,000	300	3	13.81	27.38	1.30	1.56
14	HSS	15,000	500	5	19.03	41.31	1.34	1.41
15	HSS	15,000	500	7	20.42	48.86	1.35	1.47
16	HSS	15,000	700	3	19.86	28.27	1.34	1.46
17	HSS	15,000	700	5	22.49	35.14	1.32	1.40
18	HSS	15,000	700	7	24.50	55.76	1.39	1.44
19	HSS	18,000	300	3	10.05	27.04	1.30	1.45
20	HSS	18,000	300	5	11.91	69.58	1.37	1.45
21	HSS	18,000	300	7	14.53	80.92	1.31	1.54
22	HSS	18,000	500	3	17.15	30.45	1.32	1.51
23	HSS	18,000	500	5	18.66	46.34	1.35	1.42
24	HSS	18,000	500	7	23.29	62.50	1.33	1.47
25	HSS	18,000	700	3	22.50	30.20	1.35	1.40
26	HSS	18,000	700	5	24.87	42.52	1.36	1.53
27	HSS	18,000	700	7	33.94	67.59	1.28	1.38
28	SC	12,000	300	3	6.50	28.48	1.23	1.36
29	SC	12,000	300	5	6.70	34.04	1.26	1.27
30	SC	12,000	300	7	7.56	38.52	1.25	1.26
31	SC	12,000	500	3	9.40	30.48	1.26	1.31
32	SC	12,000	500	5	9.41	34.55	1.27	1.24
33	SC	12,000	500	7	9.43	39.43	1.20	1.26
34	SC	12,000	700	3	10.56	31.48	1.31	1.46
35	SC	12,000	700	5	11.10	32.79	1.25	1.29
36	SC	12,000	700	7	11.30	35.52	1.28	1.35
37	SC	15,000	300	3	6.01	26.83	1.23	1.30
38	SC	15,000	300	5	7.04	35.33	1.21	1.25
39	SC	15,000	300	7	7.40	37.50	1.22	1.27
40	SC	15,000	500	3	8.55	29.72	1.27	1.32
41	SC	15,000	500	5	8.52	33.45	1.21	1.28
42	SC	15,000	500	7	9.52	37.95	1.18	1.24
43	SC	15,000	700	3	9.63	30.29	1.27	1.29
44	SC	15,000	700	5	9.92	33.67	1.29	1.29
45	SC	15,000	700	7	10.37	39.06	1.17	1.21
46	SC	18,000	300	3	4.80	27.02	1.22	1.29
47	SC	18,000	300	5	5.37	28.56	1.20	1.20
48	SC	18,000	300	7	5.78	35.53	1.18	1.19
49	SC	18,000	500	3	6.27	28.05	1.28	1.27
50	SC	18,000	500	5	7.72	33.09	1.26	1.26
51	SC	18,000	500	7	7.78	36.38	1.17	1.21
52	SC	18,000	700	3	7.80	29.38	1.19	1.28
53	SC	18,000	700	5	9.12	35.61	1.26	1.26
54	SC	18,000	700	7	7.70	39.83	1.16	1.29
55	SCBH	12,000	300	3	8.84	27.64	1.21	1.21
56	SCBH	12,000	300	5	9.48	30.17	1.31	1.34
57	SCBH	12,000	300	7	9.61	33.02	1.16	1.21
58	SCBH	12,000	500	3	10.61	28.74	1.30	1.30

(continued)

Table 3. (continued)

Test no.	Tool type	Speed	Feed	Thick	TF	Temp	DF (Entry)	DF (Exit)
59	SCBH	12,000	500	5	11.50	30.10	1.23	1.27
60	SCBH	12,000	500	7	11.62	41.04	1.17	1.24
61	SCBH	12,000	700	3	12.57	27.34	1.32	1.34
62	SCBH	12,000	700	5	13.23	29.41	1.27	1.34
63	SCBH	12,000	700	7	13.51	34.79	1.23	1.24
64	SCBH	15,000	300	3	7.20	28.90	1.22	1.34
65	SCBH	15,000	300	5	8.12	30.50	1.30	1.39
66	SCBH	15,000	300	7	8.50	29.05	1.13	1.20
67	SCBH	15,000	500	3	9.64	27.58	1.26	1.35
68	SCBH	15,000	500	5	10.84	28.59	1.22	1.29
69	SCBH	15,000	500	7	11.71	39.31	1.20	1.25
70	SCBH	15,000	700	3	11.44	27.37	1.25	1.43
71	SCBH	15,000	700	5	13.45	29.22	1.29	1.35
72	SCBH	15,000	700	7	14.23	33.66	1.25	1.21
73	SCBH	18,000	300	3	5.91	27.70	1.23	1.33
74	SCBH	18,000	300	5	6.57	29.84	1.27	1.27
75	SCBH	18,000	300	7	10.09	30.21	1.16	1.18
76	SCBH	18,000	500	3	7.20	26.97	1.21	1.25
77	SCBH	18,000	500	5	9.70	26.20	1.19	1.22
78	SCBH	18,000	500	7	10.01	34.24	1.15	1.24
79	SCBH	18,000	700	3	10.42	27.20	1.19	1.32
80	SCBH	18,000	700	5	11.13	27.50	1.26	1.35
81	SCBH	18,000	700	7	11.63	30.49	1.19	1.26

Speed: spindle speed (rpm), feed: feed rate (mm/min), Thick: laminate thickness (mm), TF: thrust force (N), Temp: drilling generated temperature (°C), DF: delamination factor.

Results and discussion

Experiment results

The various experimentation conditions for drilling of GFRP composites and the results for thrust force, drilling generated temperature, and DF are given in Table 3. Each test condition was run 10 times, and an average value was calculated for analyzing the results. The maximum/minimum values of temperature, the thrust force, and DF (at entry and exit) are observed in tests no: 21/77, 27/46, 18/66, and 8/75.

Based on Table 3, the lowest DF value was obtained for test 66 with 15,000 rpm, 300 mm/min, and 7 mm for the SCBH tool, which the DF quality compared with HSS and SC drilling tools in the same conditions as given in Figure 3.

The hole quality can be analyzed based on medium and higher speed. In the case of medium speed (15,000 rpm), hole quality was examined at 300 mm/min feed rate and 7 mm composite's thickness (for HSS test 12, SC test 39 and SCBH test 66 in Table 3). As described in Figure 3, the SCBH tool proposed better hole surface quality than SC and HSS. The primary types of delamination were formed in fiber pull-out, un-cut fibers, and matrix debonding. The HSS tool caused the highest drilling generated temperature and thrust force and highest delamination defects on a drilled hole in GFRP composites comparing SC and SCBH tools (Figure 3(a)) at the same drilling condition. The SCBH displayed only slight fiber pull-out and matrix debonding, and almost no uncut fibers were seen inside the hole after drilling at the same drilling condition (Figure 3(c)). Hence, this tool can be the best choice for better performance in terms of hole quality at 15,000 rpm drilling speed. For considering the higher drilling speed, the SC tool showed the high quality of drill hole at higher speed (18,000 rpm), lower feed rate (300 mm/min) and higher composite's thickness (7 mm) compared to HSS and SCBH (Figure 4). SC had the lowest thrust force (5.8 N), while HSS and SCBH had 14.5 N and 10.1 N at the same condition. The SC displayed only slight fiber pull-out and matrix debonding, and almost no uncut fibers were seen inside the hole after drilling (Figure 4(b)). Hence, the SC drill bit can be the best choice for better performance at a higher speed in terms of excellent hole quality and lower thrust force. Lower thrust force is crucial for long tool life.[50]

ANOVA analysis

ANOVA was used to identify the main factors and their interactions are statistically significant within a 95% confidence level. p-values lower than or equal to 0.05 imply that the main factor (tool type, speed, feed, thick, or the interaction) significantly affects the thrust force, temperature, and DF. Insignificant factors are eliminated when the p-value was higher than 0.05. F-value describes the variable's significance if it is higher than the critical value. p-value is calculated based on F-statistics,
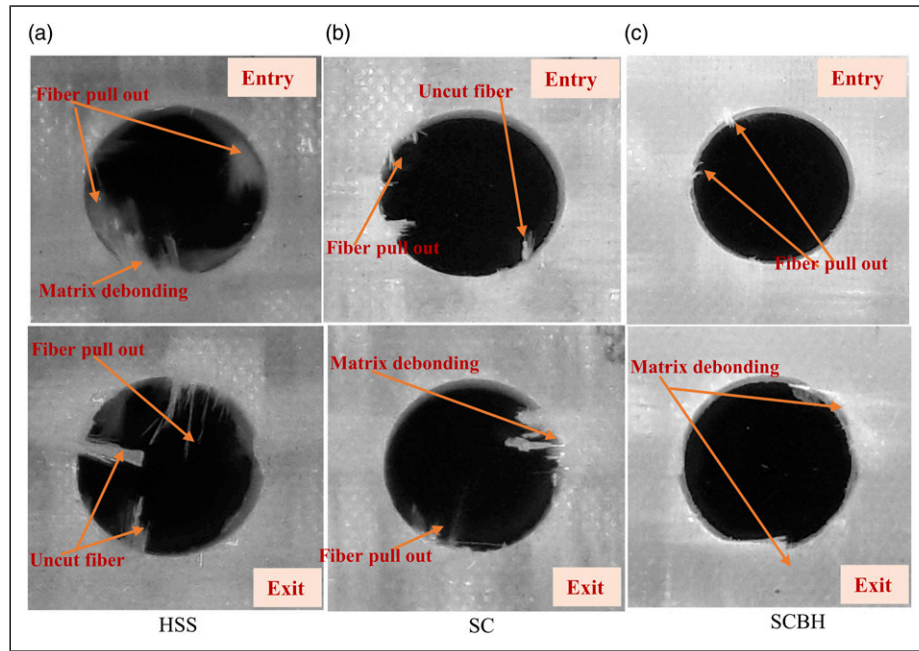
Figure 3. 3D Non-contact images of typical delamination of 7 mm thick GFRP laminate at 15,000 rpm spindle speed and 300 mm composite's thickness.
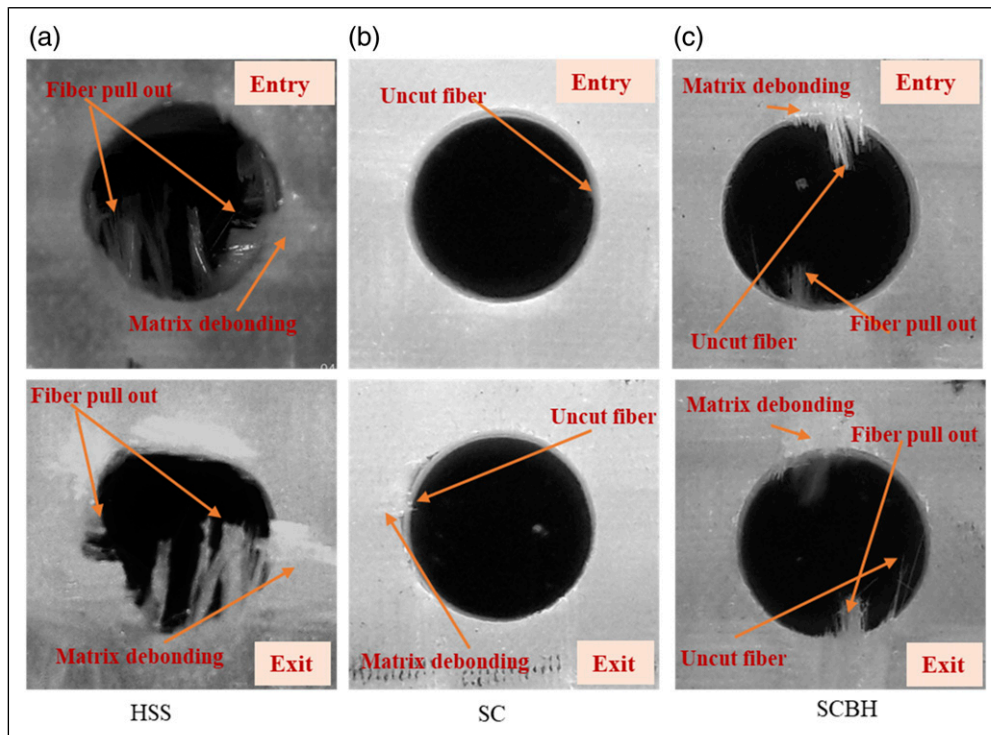

Figure 4. 3D Non-contact images of typical 7 mm thick GFRP laminate delamination at 18,000 rpm spindle speed and 300 mm/min feed rate.

which should consider with F-value. The correlation coefficient (R^2 adj) was also presented for the experimental model. Seq SS shows the variation in drilling parameters. Table 4 presents the ANOVA results for all drilling parameters and responses.

The thrust force was significantly influenced by feed rate, thickness, and tool type. Insignificant factors are eliminated when the *p*-value was higher than 0.05. There was no crucial contribution of speed found on thrust force. However, the second-order interaction with tool type (tool type and speed, tool type and feed rate, tool type, and thickness) and the third-order interaction (tool type, speed, and feed) showed the essential impact on thrust force.

Regarding the drilling generated temperature results, it can be concluded that its drilling response is statistically influenced by tool type, feed rate, and laminate thickness (as given in Table 4). Other parameters did not display a crucial impact on the

Table 4. ANOVA analysis for the thrust force, temperature, DF at entry and exit.

Drilling parameters	TF(N) seq SS	F-value	p-Value	Temp. (°C) Seq SS	F-value	p-Value	DF (entry) Seq SS	F-value	p-Value	DF (exit) Seq SS	F-value	p-Value
T	1346.25	538.88	0.00	3045.7	136.39	0.00	0.13	51.22	0.00	0.61	272.63	0.00
s	1.23	0.49	0.62	78.6	3.52	0.05	0.01	4.70	0.02	0.01	6.82	0.00
f	468.90	187.69	0.00	161.8	7.25	0.00	0.01	5.24	0.01	0.01	5.14	0.01
t	117.69	47.11	0.00	3430.9	153.64	0.00	0.04	17.71	0.00	0.04	19.97	0.00
T*s	104.44	20.90	0.00	512.0	11.46	0.00	0.00	0.92	0.47	0.02	4.95	0.00
T*f	125.90	25.20	0.00	638.0	14.28	0.00	0.00	0.91	0.48	0.01	2.44	0.08
T*t	72.27	14.46	0.00	1946.7	43.59	0.00	0.00	1.08	0.40	0.03	6.69	0.00
s*f	15.29	3.06	0.04	16.2	0.36	0.83	0.00	0.77	0.56	0.01	2.29	0.10
s*t	7.44	1.49	0.25	63.2	1.41	0.27	0.00	1.46	0.26	0.00	1.06	0.40
f*t	1.37	0.27	0.89	141.7	3.17	0.04	0.00	1.63	0.21	0.01	2.26	0.10
T*s*f	52.14	5.22	0.00	25.5	0.29	0.96	0.00	0.86	0.56	0.01	1.43	0.25
T*s*t	9.54	0.95	0.50	210.7	2.36	0.06	0.01	1.41	0.26	0.02	2.93	0.03
T*f*t	6.98	0.70	0.68	452.2	5.06	0.00	0.02	2.30	0.07	0.02	3.24	0.02
s*f*t	2.92	0.29	0.95	35.4	0.40	0.90	0.00	0.41	0.90	0.01	1.45	0.25
R^2 (adj)	95.75%			91.83%			66.74%			89.69%		

T: tool types; s: speed; f: feed rate; t: thickness; Seq SS: Sequential sums of squares; * interaction between the parameters.
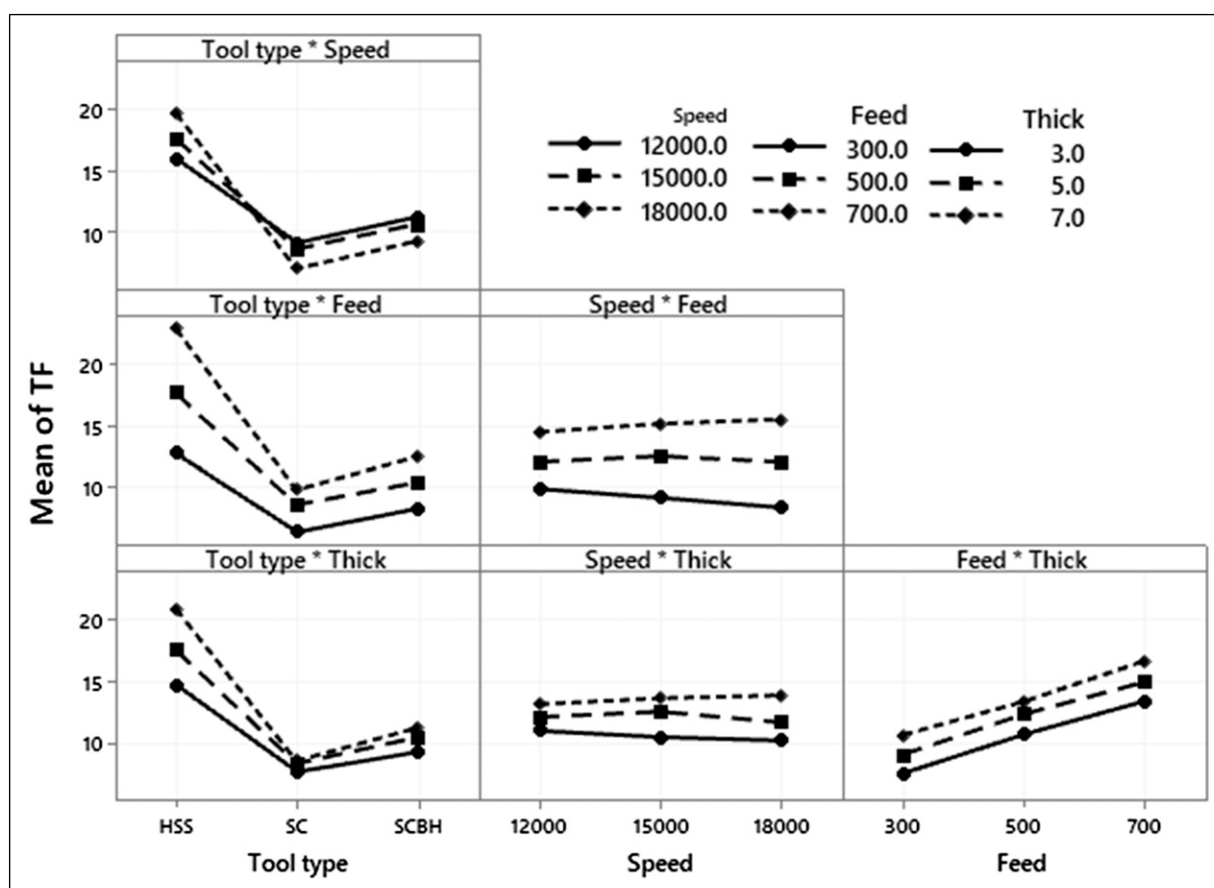
Figure 5. Interaction graph for thrust force.

temperature. Those parameters showed a significant contribution in second-order interaction with tool type (tool type and speed; tool type and feed rate; tool type and thickness; feed rate and thickness) and the third-order interaction (tool type, feed rate, and thickness).

As shown in Table 4, both delamination factors (entry and exit) were affected by all main drilling parameters. The tool types showed the highest significance, followed by thickness. There was no significant impact on the interaction between the parameters on DF (entry); however, second-order interaction (tool type and speed; tool type and thickness) and third-order interaction (Tool type, speed and feed rate; tool type, feed rate, and thickness) showed a significant effect of DF (exit). The
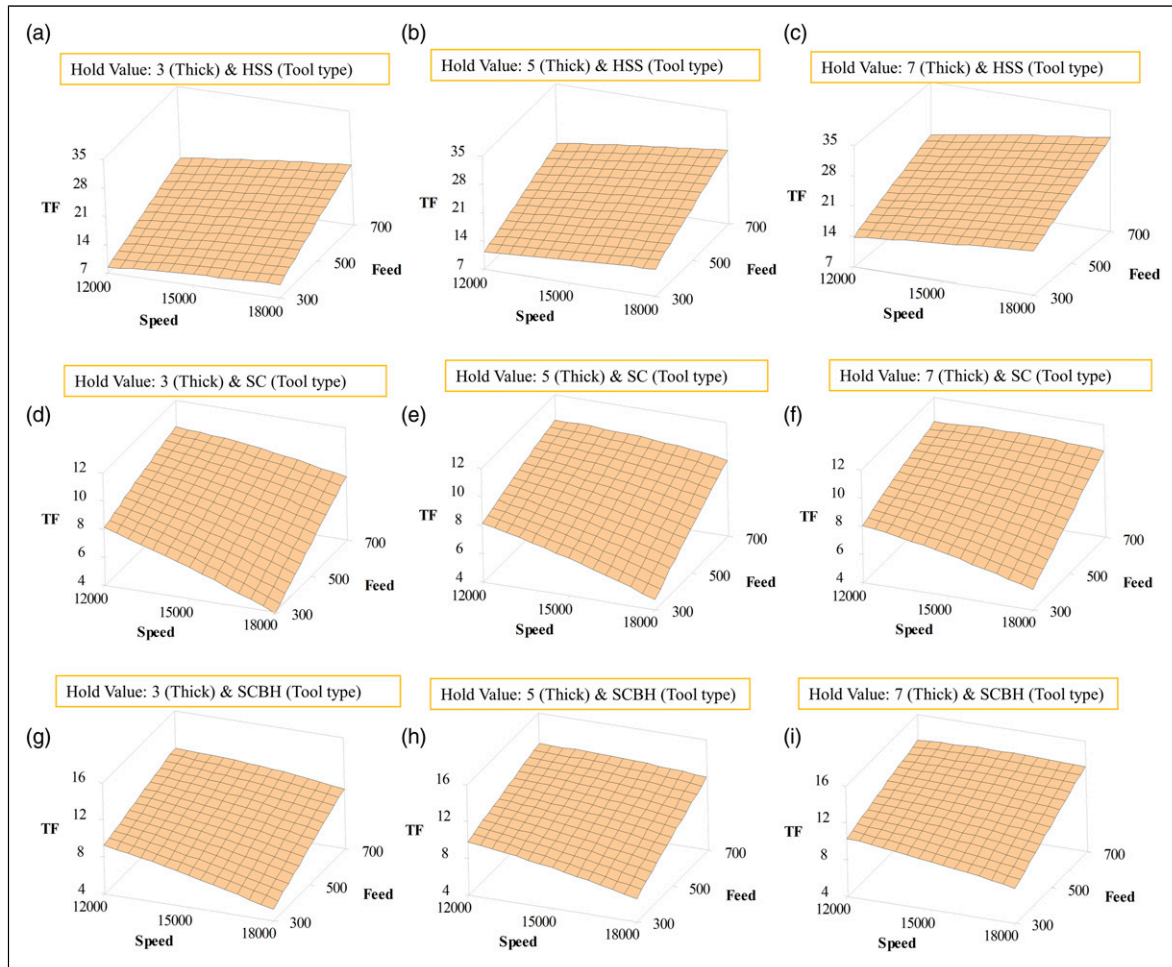
Figure 6. Surface plot of TF versus feed and speed, a), b), and c) for HSS tools, d), e) and f) for SC tools, and g), h), and i) for SCBH tool with varying thickness.

main reason for the effect of tool type and speed on DF is explained later on considering the effect of chip residual on drilling performance.

Based on all the significant drilling parameters presented in Table 4, the thrust force can be controlled by the tool type, feed rate, and thickness. The drilling generated temperature can be reduced by careful selection of tool type and thickness of laminates. Low delamination in the holes' entrance and exit can be reduced by optimum selection of all major factors.

RSM analysis of drilling performance parameters

The graph in Figure 5 displays an interaction plot matrix for the mean of thrust force, which shows no interaction (parallel lines) for speed * feed, speed * thick, and feed * thick, but other combinations presented the interaction. The feed rate was a more significant variable compared to speed and thickness for thrust force. The speed * feed graph that all drilling tools showed slightly different trends in which SC and SCBH showed the lower thrust force at high speed compared to HSS tools.

For the HSS tool, thrust force increased with speed, feed rate, and thickness (Figure 6(a)–(c). SC and SCBH tools offered almost similar thrust force responses for feed rate and thickness; however, the effect of speed rate was contrary for the HSS tool (Figure 6(d)–(i)). The thrust force was found to increase with a rise in feed rate. However, it decreased when the drilling speed increased for SC and SCBH tools (Figure 6(d)–(i)). The composite thickness had a negligible impact on thrust force for SC and SCBH tools at low spindle speed but insignificant at the higher speed.

Moreover, drilling at a higher speed showed benefits in these tools compared to the HSS tool for lowering the thrust force (Figure 5). HSS has the increasing trend for trust force while drilling speed increases due to exceeding the optimum drilling conditions for GRFP composites; therefore, the thrust force is increasing contrary to SC and SCBH drill. Considering that all the other parameters are the same for drill bits, the hardness of the drill bit or its coating materials is the most crucial parameter.

It has been observed that the thrust force of HSS drills is higher when compared with SC and SCBH drills because HSS drills are less hard and wear out more effectively.[17] The GFRP composite chip residual on the HSS twist drill bit was detected, while there was almost no chip residual on the SC. The GFRP composite residual not only increases the frictional force between the tool bit and cutting zone by its abrasive nature, but it may also cause rapid tool wear on HSS, which is one of the reasons for higher thrust force for high-speed drilling of GFRPs using HSS tool.[51,52] The high tool wear reduced the edge
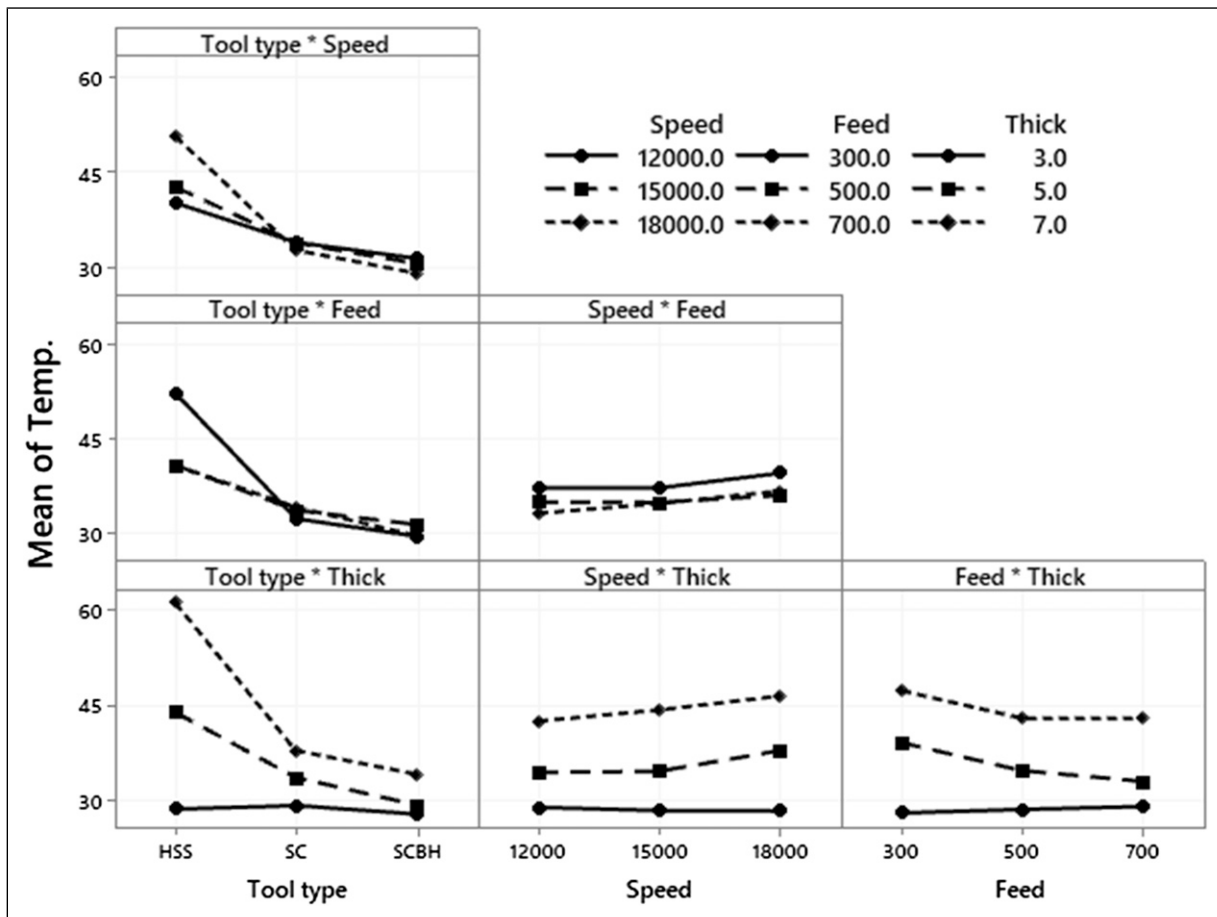
Figure 7. Interaction graph for drilling generated temperature.

sharpness of the tool bit and generated higher thrust force from the uncut thickness of the GFRP laminates.[51,52] Therefore, the GFRP composites' thickness significantly influenced the thrust force, and the thicker composite generated higher thrust force, thus increasing the delamination supported by Table 3 and Figure 6. The lower thrust force generated from SC and SCBH tools than the HSS tool may be due to higher speed, where the high material removal rate compensated the downward thrust force at a higher feed rate. Tool wear of the HSS drill bit is main factor that causes the thrust force to increase, where SC and SCBH drill bit has the advantage of higher material hardness, thus making them less prone to tool wear and retained edge sharpness more effectively.[53] SCBH tool showed a slightly higher thrust force than SC tools (Table 3) due to the Balinit® Helica coating. It may be due to higher residue produced by SCBH, as higher residue causes higher frictional force, resulting in ameliorate thrust force.[54] Since glass fiber reinforcement is an abrasive and hard material, Balinit Helica had to be used due to the coating's AlCrN based properties that offer better abrasion resistance, lower adhesion tendency, and lower friction.[55] This coating and most of the coatings (TiAlN, TiN and diamond) are ceramic, making it vulnerable to mechanical impacts caused by intermittent cuts of the fibers.[56] Abrasion can cause wear on the edges.[57] However, Balinit Helica coating is more resistant to abrasion, and drilling still damages it despite its abrasion resistance.[54,56]

Figure 7 displays the interaction graph for drilling generated temperature. For HSS, the temperature was found to increase with the rise of speed and thickness which can be seen from tool-type * speed and tool type * thick interaction graphs. However, the feed displayed an opposite response to the temperature. The temperature was almost constant, although a small decrement was observed when speed increased for SC and SCBH tools. The temperature is often related to a high feed rate that develops high thrust force during drilling, which increases the frictional force between the cutting tool and the cutting material. However, with a high feed rate, the cutting time may be reduced with a faster traveling time. The tool type and thickness were other vital factors that displayed a crucial impact on the temperature. The temperature displayed an increasing trend with augmentation of the laminate thickness for all tested tools. Other combinations of interactions did not show any signs.

For the HSS tool, the high temperature was seen at a low feed rate (Figure 8(a)–(c)). The feed rate influence on the temperature using the SC and SCBH tools presented a slightly different behavior than the HSS (Figure 8(d)–(i)). The temperature was slightly increased with a rise in feed rate for SC and SCBH tools. The higher temperature was produced by HSS tools at higher speed compared to SC and SCBH tools which had lower temperature at higher speed. The temperature generated during drilling is crucial for polymer composites. The epoxy has a degradation temperature between 120°C – 270°C.[39] In this study, the generated temperature was found lower than 120°C. The thrust force was found directly relative to
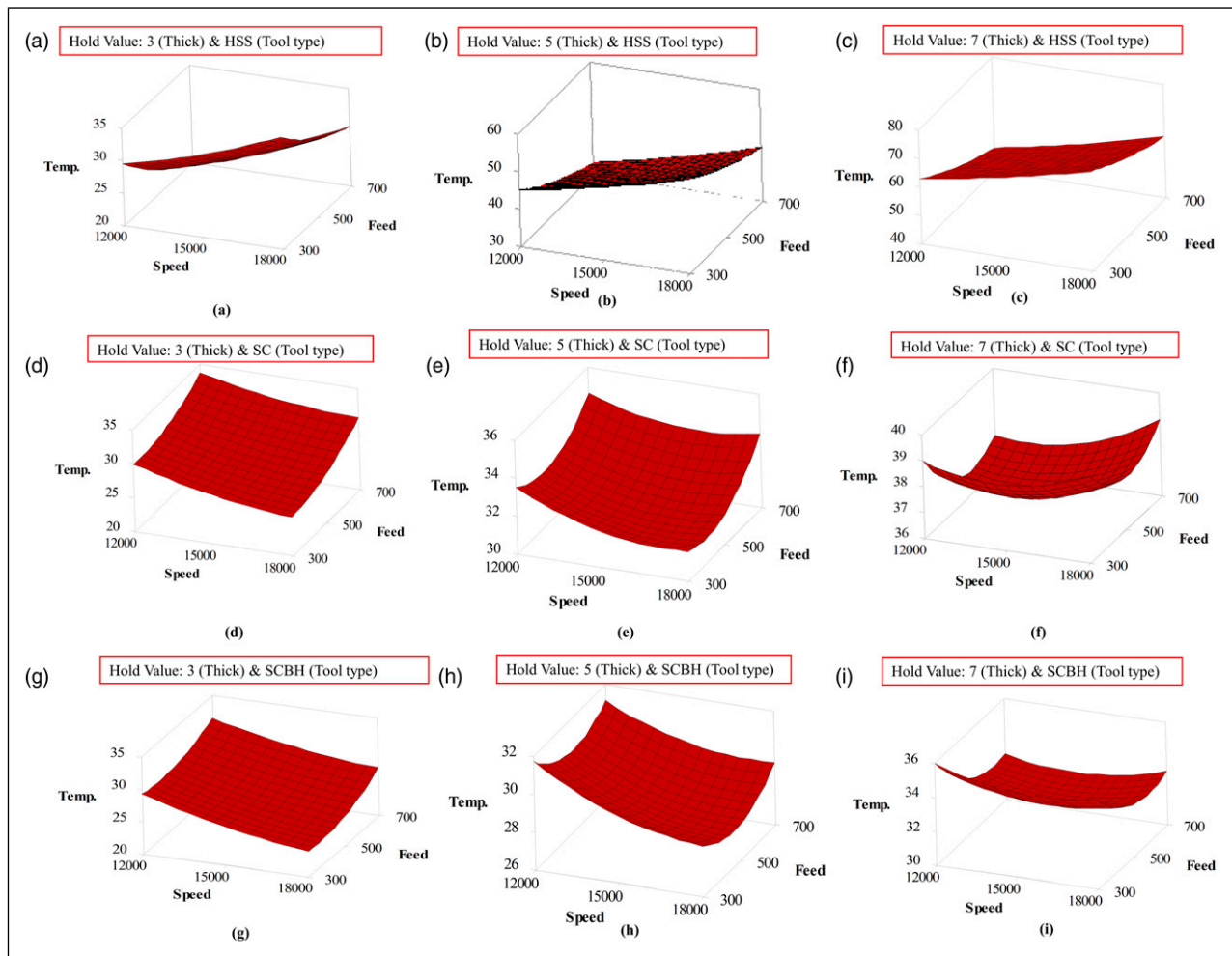
Figure 8. Surface plot of temperature versus feed and speed, a), b), and c) for HSS tools, c), d), e), and f) for SC tools, and g), h), and i) for SCBH tool with varying thickness.

the temperature (Table 3, tests 27 and 46). Higher temperatures were noticed at a higher thrust force (Table 3, test 21, 24, and 27). The heat generated by friction between the tools and composite dissipates by the composite, the chips, and the atmosphere.[58] Low thermal conductivity materials produce high heat generation by preventing heat dissipation during the drilling operation.[25] Therefore, HSS tools generated higher temperatures than SC and SCBH during the drilling. Another reason for lower temperature generation for SC and SCBH than HSS may be their higher hot hardness and lower thermal expansion coefficient values due to presence of higher carbon and tungsten, or presence of coating material. These tools absorbed and diffused heat faster than the HSS tool and coupled with its helical flute design of the drill bit, assisted in drawing out the cutting chip while diffusing heat from the cutting tool and the cutting zone. The low thermal conductivity of HSS caused higher temperatures at the cutting zone compared to other drill bit grades.[59]

Concerning the DF, Figure 9(a) and 10 presented a main effect graph for the entry DF. It can be seen that all main drilling parameters have a crucial effect on the entry DF. The DF at the entrance was found to decrease with raising speed from 12,000 rpm to 18,000 rpm; this drop was significant for SC and SCBH tools (Figure 10). DF (entry) can be reduced, dropping the feed rate (Figure 10). Thickness showed a slightly different response; initially, the DF at entry was rising when thickness increased from 3 mm to 5 mm, followed by declination at 7 mm laminate thickness (Figure 9(a)). For all tested drilling conditions, SC and SCBH tools had a lower entry DF than the HSS tool. Test 66, as shown in Table 3, showed the lowest DF at the entrance, which was approximately 1.13 when drilling was performed by SCBH tool at speed (15,000 rpm), feed (300 mm/min), and thickness (7 mm), (Table 3, 66) as shown in Figure 3(c). Thrust force and temperatures at this delamination value were 8.5 N and 29.1°C, respectively. The highest entry delamination was around 1.39 for the HSS tool at 15,000 rpm, 700 mm/min, and 7 mm (as given in Table 3 in test 18), as shown in Figure 3. The thrust force and the temperature were recorded at around 24.5 N and 55.8°C, respectively. Considering the lower and higher DF entry conditions, higher thrust force and higher temperatures cause higher delamination. As shown in Figure 4, SC displayed excellent drill hole quality (entry) at higher speed, lower feed rate and higher thickness of composite (Table 3, test 48) compared to HSS (Table 3, test 21) and SCBH (Table 3, test 75) at identical conditions.

Similar behavior was found for the DF at the exit (as described in Figures 9(b) and 11). The DF at the exit was higher than at entry for all tested drilling parameters (Figure 3). A strong impact of the main drilling parameters on the exit DF can be seen.
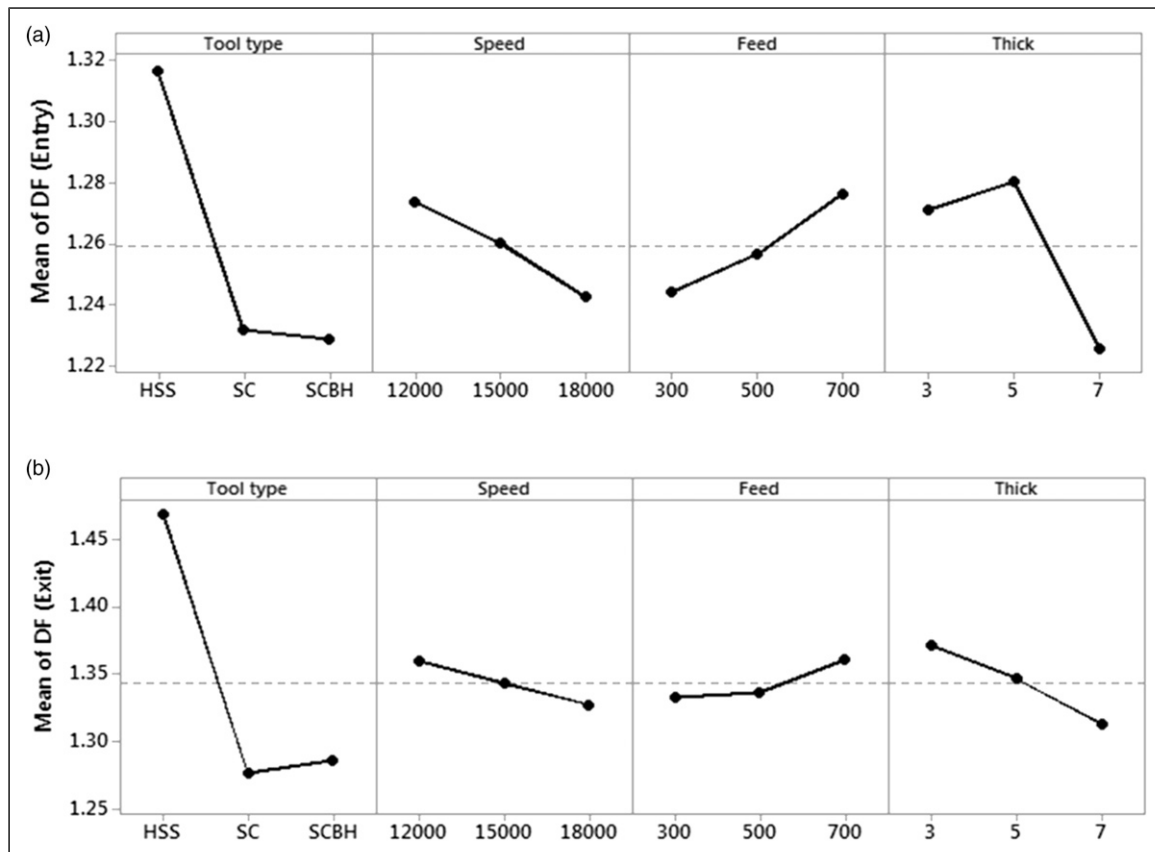
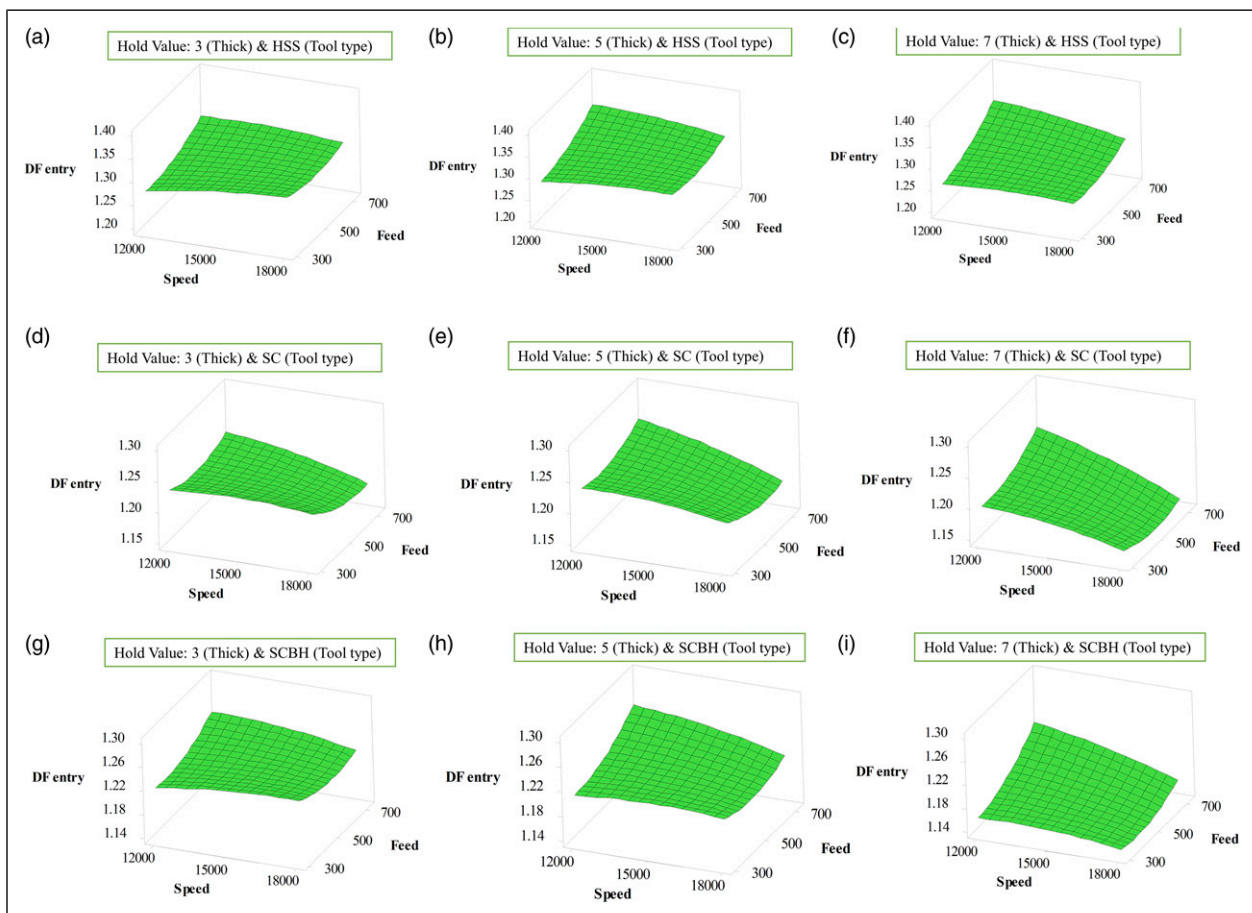**Figure 9.** Main effects plot for (a) entry DF, and (b) DF exit.

Figure 10. Surface plot of DF (Entry) vs feed and speed, a), b), and c) for HSS tools, d), e) and f) for SC tools, and g), h), and i) for SCBH tool with varying thickness.
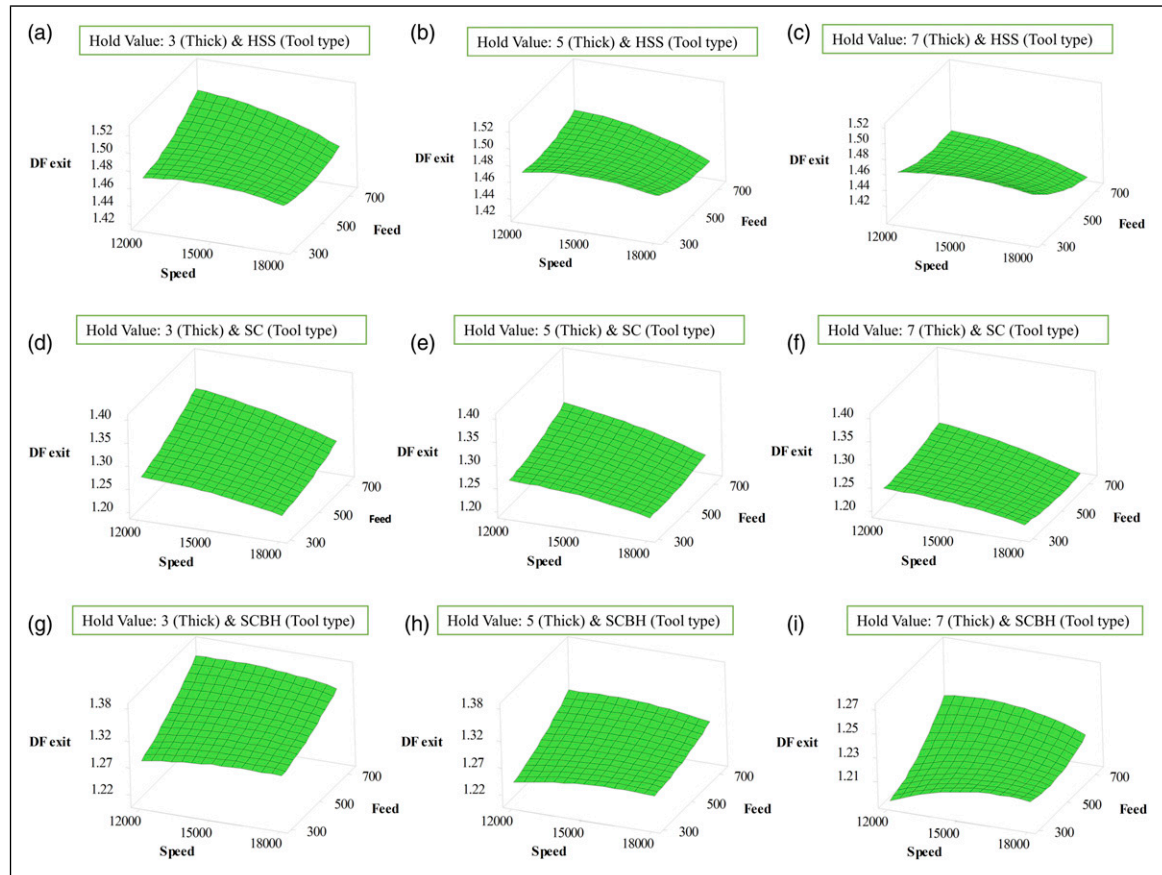
Figure 11. Surface plot of DF (Exit) vs feed and speed, a), b), and c) for HSS tools, d), e) and f) for SC tools, and g), h), and i) for SCBH tool with varying thickness.
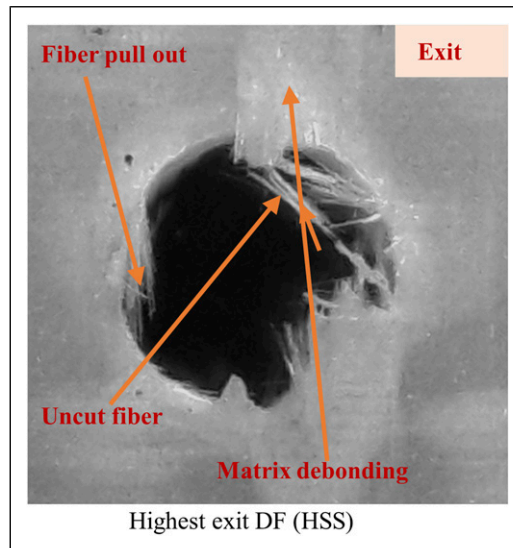

Figure 12. a) highest DF (Exit) at 12,000 rpm, 700 mm/min, and 5 mm for HSS.

The DF at exit found abridging when speed turns up from 12,000 rpm to 18,000 rpm; however, the SCBH tool showed a slightly opposite response (Figure 11). A similar response was found for thickness; it declined with increasing laminate thickness (Figure 9(b)). In the case of feed rate, it was noticed to climb with the raising of feed rate (Figure 11). SCBH tools showed lower exit DF for all tested drilling conditions than HSS and SC tools. Test 75, as shown in Table 3, had the exit DF, which was around 1.18 for the SCBH tool at 18,000 rpm, 300 mm/min, and 7 mm (Figure 4(c)). The thrust force and temperature, nearly 10.1 N and 30.2°C, respectively, were at this drilling condition. As shown in Figure 4, SC displayed excellent drill hole quality (exit) at higher speed, lower feed rate and higher thickness of composite (Table 3, test 48) compared
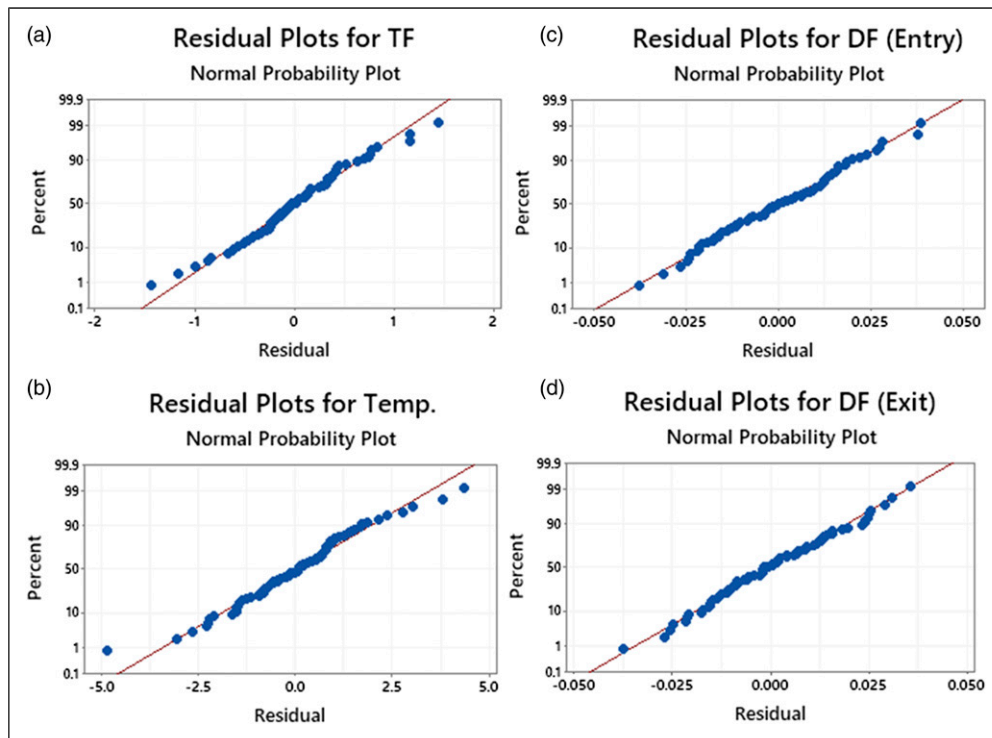
Figure 13. Residual plots: (a) Thrust force, (b) drilling generated temperature, (c) DF (entrance), and (d) DF (exit).

to HSS (Table 3, test 21) and SCBH (Table 3, test 75) at identical conditions. SCBH showed higher uncut fiber and fiber pull out compared to the SC tool, although matrix debonding was almost the same for both tools (Figure 4(b) and (c)). The highest DF was 1.57 for HSS tools at 12,000 rpm, 700 mm/min, and 5 mm (as given in Table 3 in test 8 and Figure 12(a)). The thrust force and temperature at this condition were around 19 N and 29.6°C. It can be concluded that the DF has a critical relation with the thrust force and temperature during the GFRP laminate drilling. When the thrust force increased, the drill entry DF increased due to high push-down force at the higher feed rates, which resulted in the tool bit forcing through the GFRP material rather than cutting through it. The matrix starts to fracture and chip, which leads to fiber out. Similarly, when the temperature exceeds the range of 46°C, the matrix will start to disintegrate and cause higher delamination due to premature glass fiber exposure when the matrix disintegrated.[60] Excellent drill hole quality can be achieved using SC drill bit due to lower thrust force than SCBH and HSS (Figure 4).

Optimization of the drilling performance of glass fiber reinforced polymer

As shown in Figure 13, residual plots for thrust force, drilling generated temperature, DF (entrance), and DF (exit), the normal probability plots for all drilling performances showed a similar trend with best fitted to the linear line. It shows the model used is useful to design the experiment, and results can be reasonable, which can be used to examine the drilling performance of the GFRP composite.

The following regression equations (3)–(6) for thrust force, drilling generated temperature, and DF (entrance and exit) were developed using RSM to predict the drilling performance, where T: tool types, s: speed, f: feed rate, t: thickness.

$$
\begin{aligned}
TF = \, &17.19 - 18.96\,T + 1.67\,s + 4.96\,f + 2.92\,t + 5.822\,T*T - 0.222\,s*s - 0.088\,f*f - 0.039\,t*t - 1.442\,T*s \\
&- 1.505\,T*f - 1.062\,T*t + 0.635\,s*f + 0.377\,s*t + 0.040\,f*t
\end{aligned}
$$

$$(3)$$

$$
\begin{aligned}
Temp. = \, &29.9 - 8.92\,T + 2.14\,s - 9.79\,f + 17.90\,t + 3.97\,T*T + 0.66\,s*s + 1.17\,f*f + 0.94\,t*t - 3.263\,T*s \\
&+ 2.829\,T*f - 6.631\,T*t + 0.301\,s*f + 1.142\,s*t + 1.364\,f*t
\end{aligned}
$$

$$(4)$$

$$
\begin{aligned}
DF(entry) = \, &1.3370 - 0.1604\,T + 0.0287\,s + 0.0009\,f + 0.1137\,t + 0.03981\,T*T - 0.00407\,s*s + 0.00315\,f*f \\
&- 0.03185\,t*t - 0.00806\,T*s - 0.00417\,T*f - 0.00917\,T*t - 0.00250\,s*f - 0.00306\,s*t + 0.00778\,f*t
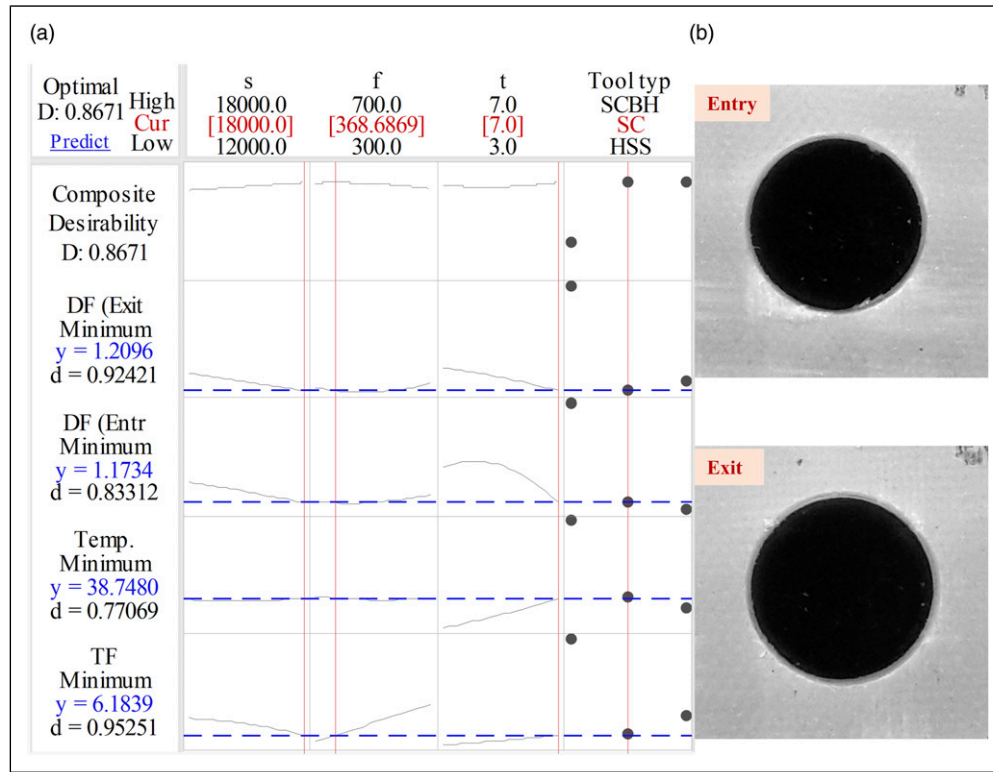\end{aligned}
$$

$$(5)$$

Figure 14. a) Optimization plot and b) drilled holes quality (Table 3, test 48).

$$DF(exit) = 1.860 - 0.4744\,T - 0.0157\,s - 0.0119\,f + 0.0391\,t + 0.0989\,T*T - 0.0006\,s*s + 0.0089\,f*f$$
$$- 0.0050\,t*t + 0.00556\,T*s + 0.00972\,T*f - 0.02083\,T*t - 0.00833\,s*f + 0.00333\,s*t - 0.00639\,f*t$$

$$(6)$$

Figure 14(a) represents the optimization plot for GFRP composite drilling. It can highlight that the best drilling condition is tool type, speed, feed rate, and thickness at levels 300, 18,000, 7, and SC, respectively.

Drilling generated temperature and thrust force have the lower and higher desirability score (0.77,069 and 0.95,251, respectively) than composite desirability (0.8671) because the predicted responses of 34.7480 and 6.1839 are higher than the target of minimum 26.2°C and 4.8 N, respectively, but still inside the acceptable range. The drilled hole's quality at 18,000 rpm, 300 feed rate and 7 mm thickness (Table 3, test 48) is given in Figure 14(b), with DF's value at the entrance and exit as 1.18 and 1.19, respectively. The thrust force and drilling generated temperatures were 5.7 N and 35.5°C, respectively. It can be stated that the SC tool could be most suitable for better drilling performance for GFRP composite at a higher speed compared to the HSS and SCBH drill bits.

Validation was performed to determine the accuracy of the model. 10 random sets of drilling parameters were selected to perform the validation experiments for each drill bit grade. Three sets out of range parameter validation experiments were included in the random sets to determine the parametric adequacy range of the model. The prediction model was developed using RSM for each drill tool, shown from equations (7) to (12). The percentage error is calculated using equation (13). DF, f, s, and t are the delamination factor, feed rate, speed, and thickness of composites. The subscript exp. and the model represents the validation experiment result and the model calculation result

$$DF\,(Entry)_{HSS} = 1.011 + 0.000019\,s + 0.000028\,f + 0.0707\,t - 0.00790\,t^2 - 0.000001\,s*t + 0.000019\,f*t \quad (7)$$

$$DF\,(Exit)_{HSS} = 1.532 - 0.000002\,s - 0.000107\,f + 0.0060\,t\,0.00122\,t^2 + 0.000001\,s*t - 0.000011\,f*t \quad (8)$$

$$DF\,(Entry)_{SC} = 1.081 + 0.000013\,s - 0.000038\,f + 0.0647\,t - 0.00790\,t^2 - 0.000001\,s*t + 0.000019\,f*t \quad (9)$$

$$DF\,(Exit)_{SC} = 1.440 - 0.000007\,s + 0.000003\,f - 0.0085\,t - 0.00122\,t^2 + 0.000001\,s*t - 0.000011\,f*t \quad (10)$$

$$DF\,(Entry)_{SCBH} = 1.069 + 0.000013\,s - 0.000016\,f + 0.0619\,t - 0.00790\,t^2 - 0.000001\,s*t + 0.000019\,f*t \quad (11)$$

$$DF\,(Exit)_{SCBH} = 1.343 + 0.000002\,s + 0.000015\,f - 0.0152\,t - 0.00122\,t^2 + 0.000001\,s*t - 0.000011\,f*t \quad (12)$$

Table 5. Result of validation and adequacy test.

Drilling parameters			DF (Entry)			DF (Exit)		
Speed (rpm)	Feed rate (mm/ min)	Thickness (mm)	Validation experiment	Model calculation	% Error	Validation experiment	Model calculation	% Error
HSS drill bit								
9000	800	7	1.60	1.35	−15.63	1.79	1.41	−21.23
10000	300	5	1.63	1.34	−17.79	1.68	1.51	−10.12
13000	500	5	1.45	1.41	−2.76	1.42	1.49	4.93
15000	300	3	1.52	1.42	−6.58	1.69	1.51	−10.65
15000	600	7	1.51	1.39	−7.95	1.29	1.48	14.73
15000	700	3	1.46	1.45	−0.68	1.42	1.45	2.11
16000	300	7	1.43	1.36	−4.90	1.28	1.54	20.31
17000	600	3	1.71	1.48	−13.45	1.42	1.47	3.52
18000	400	5	1.53	1.47	−3.92	1.14	1.52	33.33
20000	200	5	1.35	1.47	8.89	1.13	1.55	37.17
SC drill bit								
9000	800	7	1.68	1.28	−23.81	1.59	1.26	−20.75
10000	300	5	1.55	1.30	−16.13	1.58	1.33	−15.82
13000	500	5	1.34	1.34	0.00	1.48	1.32	−10.81
15000	300	3	1.24	1.36	9.68	1.45	1.33	−8.28
15000	600	7	1.33	1.29	−3.01	1.49	1.28	−14.09
15000	700	3	1.38	1.37	−0.72	1.69	1.32	−21.89
16000	300	7	1.20	1.27	5.83	1.48	1.30	−12.16
17000	600	3	1.44	1.39	−3.47	1.50	1.32	−12.00
18000	400	5	1.12	1.37	22.32	1.26	1.31	3.97
20000	200	5	1.08	1.37	26.85	1.15	1.31	13.91
SCBH drill bit								
9000	800	7	1.60	1.26	−21.25	1.79	1.21	−32.40
10000	300	5	1.63	1.28	−21.47	1.68	1.29	−23.21
13000	500	5	1.45	1.32	−8.97	1.42	1.31	−7.75
15000	300	3	1.52	1.34	−11.84	1.70	1.36	−20.00
15000	600	7	1.51	1.28	−15.23	1.29	1.27	−1.55
15000	700	3	1.46	1.36	−6.85	1.42	1.35	−4.93
16000	300	7	1.43	1.25	−12.59	1.29	1.30	0.78
17000	600	3	1.71	1.38	−19.30	1.42	1.36	−4.23
18000	400	5	1.53	1.36	−11.11	1.15	1.35	17.39
20000	200	5	1.35	1.36	0.74	1.13	1.36	20.35

$$Percentage\ of\ error = \frac{DF_{exp.} - DF_{model}}{DF_{exp.}} \times 100 \qquad (13)$$

The result of the validation test is shown in Table 5. From the validation and adequacy test result for the HSS twist drill bit, DF (entry) showed a maximum 17.8% error compared to the experiment result, while DF (exit) the model in equation (8) showed a maximum 37.2% error compared to DF (exit) the experiment result. SC twist drill bit developed model in equation (9) and equation (9) showed a maximum 26.8% error for DF (entry) and 21.9% error for DF (exit) compared to the experiment result. In comparison, SCBH twist drill bit developed model showed the highest 21.5% error for DF (entry) and 32.4% error for DF (exit). The error between the results from the models and the experiment was considered due to external factors such as machine vibration, tool wear, human error, etc., that are not considered. The adequacy test showed that the model might be utilized to predict drilling parameters in the ranges.

Conclusions

The drilling operation was done on the GFRP composite using various main input parameters such as tool type, speed, feed rate, and composite thickness. The thrust force, drilling generated temperature, and DF (at entry and exit) were examined for the drilling performance of GFRP composites. The HSS, SC, and SCBH twist drill bits were used to drill the hole at a high-speed range (12,000-18,000 rpm).

1. The results showed that the thrust force could be minimized significantly by reducing the speed, feed, and thickness when the HSS drill bit was used. However, SC and SCBH showed a different response for thrust force at variation speed, especially SC, which showed the lowest thrust force at a higher speed.
2. The drilling-generated temperature can be minimized at a lower speed and thickness. The temperature was almost constant with the speed and feed rate variation for SC and SCBH tools. HSS tool presented a decreasing trend (temperature) when the feed rate rose from 300   mm/min to 700   mm/min.
3. ANOVA and RSM were used to examine the drilling process of the GFRP composite. ANOVA analysis presents that all the input parameters, except speed and second-order interaction with tool type, substantially influence thrust force. The temperature, tool type, and thickness had a significant impact, besides the second-order interaction of the major parameters with tool type. The DF at entry and exit were found to be affected by the main parameters. The selection tool type had a critical impact on the DF at the entrance and exit compared to other drilling parameters.
4. The highest DF was found for HSS, and the lowest was for the SC and SCBH drill tool, which showed the benefit of using higher drilling speed for GFRP composite. However, HSS showed higher drilling temperature at low speed, high feed rate, and low thickness of GFRP but when drilling speed increased, delamination of HSS also increased. The type of delamination was matrix debonding, uncut fiber, and fiber pull out during drilling operation.
5. From RSM analysis, the regression equations were generated to predict the thrust force, temperature, and DF (at entry and exit). The best drilling performance was achieved by using the SC tool at a higher speed (18,000 rpm), higher thickness (7   mm), and lower feed rate (300   mm/min). The DF at entry and exit was found around 1.18 1 and 1.19, respectively, at 5.7   N (thrust force) and 35.5°C (temperature).

In conclusion, higher composite's thickness with SC drill bit is recommended most suitable for drilling GFRP composite at a higher speed and lower feed rate than the HSS and SCBH . SCBH drill bits may also be utilized for a good quality hole, although it had higher thrust force than SC, which reduce tool life. The drilling process and performance method used in this study is recommended to manufacture GRFP laminates in aerospace, marine, and automotive industries, especially structural applications.

Acknowledgements

Authors' contributions

Khurshid Malik: Methodology, Writing - original draft, Writing - review & editing. Faiz Ahmad: Supervision. Woo Tze Keong: Data curation. Ebru Gunister: Final review & editing.

Declaration of conflicting interests

The author(s) declared no potential conflicts of interest with respect to the research, authorship, and/or publication of this article.

Funding

Availability of data and material

Raw data is available with author on request.

Consent for publication

All authors have approved the manuscript and agree with its submission to Polymers and Polymer Composites.

ORCID iDs

Faiz Ahmad https://orcid.org/0000-0002-8819-0747
Ebru Gunister https://orcid.org/0000-0002-7797-604X

References

1. Palanikumar K, Latha B, Senthilkumar VS, et al. Analysis on drilling of glass fiber–reinforced polymer (GFRP) composites using grey relational analysis. *Mater Manufacturing Process* 2012; 27: 297–305. DOI: 10.1080/10426914.2011.577865.
2. Malik K, Ahmad F, Yunus NA, et al. The effects of graphene hybridization on mechanical properties of GFRP composites. In: AIP Conference Proceedings 2021, Langkawi, Malaysia, 7-8 February 2021. AIP Publishing LLC, 020023.
3. Campos Rubio J, Panzera T, Abrao A, et al. Effects of high speed in the drilling of glass whisker-reinforced polyamide composites (PA66 GF30): statistical analysis of the roughness parameters. *J Compos Mater* 2011; 45: 1395–1402.

4. Latha B and Senthilkumar VS. Fuzzy rule based modeling of drilling parameters for delamination in drilling GFRP Composites. *J Reinforced Plastics Composites* 2009; 28: 951–964. DOI: 10.1177/0731684407087570.

5. Feito N, Díaz-Álvarez J, Díaz-Álvarez A, et al. Experimental analysis of the influence of drill point angle and wear on the drilling of woven CFRPs. *Materials* 2014; 7: 4258–4271, DOI: 10.3390/ma7064258.

6. Giasin K, Ayvar-Soberanis S and Hodzic A. An experimental study on drilling of unidirectional GLARE fibre metal laminates. *Compos Struct* 2015; 133: 794–808, DOI: 10.1016/j.compstruct.2015.08.007.

7. Das K, Kamaruzzaman S, Middya TR, et al. Study of variation of thermal diffusivity of advanced composite materials of E-glass fibre reinforced plastic (GFRP) in temperature range 5–300 K. *Bull Mater Sci* 2009; 32: 89–92.

8. Isbilir O and Ghassemieh E. Delamination and wear in drilling of carbon-fiber reinforced plastic composites using multilayer TiAlN/TiN PVD-coated tungsten carbide tools. *J Reinforced Plastics Composites* 2012; 31: 717–727. DOI: 10.1177/0731684412444653.

9. Jia Z, Chen C, Wang F, et al. Analytical study of delamination damage and delamination-free drilling method of CFRP composite. *J Mater Process Tech* 2020; 282: 116665, DOI: 10.1016/j.jmatprotec.2020.116665.

10. Khashaba UA and El-Keran AA. Drilling analysis of thin woven glass-fiber reinforced epoxy composites. *J Mater Process Technol* 2017; 249: 415–425, DOI: 10.1016/j.jmatprotec.2017.06.011.

11. Kilickap E. Investigation into the effect of drilling parameters on delamination in drilling GFRP. *J Reinforced Plastics Composites* 2010; 29: 3498–3503. DOI: 10.1177/0731684410386271.

12. Gaitonde VN, Karnik SR, Rubio JC, et al. Analysis of parametric influence on delamination in high-speed drilling of carbon fiber reinforced plastic composites. *J Mater Process Tech* 2008; 203: 431–438, DOI: 10.1016/j.jmatprotec.2007.10.050.

13. Işık B and Ekici E. Experimental investigations of damage analysis in drilling of woven glass fiber-reinforced plastic composites. *Int J Adv Manufacturing Tech* 2010; 49: 861–869. DOI: 10.1007/s00170-009-2440-x.

14. Latha B, Senthilkumar VS and Palanikumar K. Modeling and optimization of process parameters for delamination in drilling glass fiber reinforced plastic (GFRP) composites. *Machining Sci Tech* 2011; 15: 172–191. DOI: 10.1080/10910344.2011.579802.

15. Priya IIM and Vinayagam BK. Investigation of drilling parameters using grey relational analysis and response surface methodology of biaxial glass fibre reinforced with modified epoxy resin composite. *Int J Polym Sci* 2018; 12. Article. DOI: 10.1155/2018/8629894.

16. Prakash M and Dhar P. Investigation on the effect of drilling parameters on the tool wear and delamination of glass fibre-reinforced polymer composite using vibration signal analysis. *J Compos Mater* 2018; 52: 1641–1648. Article. DOI: 10.1177/0021998317728109.

17. Mudhukrishnan M, Hariharan P and Palanikumar K. Measurement and analysis of thrust force and delamination in drilling glass fiber reinforced polypropylene composites using different drills. *Measurement* 2020; 149: 10. Article. DOI: 10.1016/j.measurement.2019.106973.

18. Sorrentino L, Turchetta S and Bellini C. In process monitoring of cutting temperature during the drilling of FRP laminate. *Compos Struct* 2017; 168: 549–561. Article. DOI: 10.1016/j.compstruct.2017.02.079.

19. Mohan N, Kulkarni S and Ramachandra A. Delamination analysis in drilling process of glass fiber reinforced plastic (GFRP) composite materials. *J Mater Process Tech* 2007; 186: 265–271.

20. Heidary H, Mehrpouya MA, Saghafi H, et al. Critical thrust force and feed rate determination in drilling of GFRP laminate with backup plate. *Struct Eng Mech* 2020; 73: 631–640. Article. DOI: 10.12989/sem.2020.73.6.631.

21. Murthy BRN, Vijay GS, Narayan S, et al. Mechanical modelling and simulation of thrust force in drilling process in GFRP composite laminates: A novel system dynamics approach. *Cogent Eng* 2019; 6: 12. Article. DOI: 10.1080/23311916.2019.1706981.

22. Jayabal S and Natarajan U. Influence of cutting parameters on thrust force and torque in drilling of E-glass/polyester composites. *Indian J Eng Mater Sci (Ijems)* 2010; 17(6): 463–470.

23. Woo TK, Ahmad F, Sharif S, et al. Effects of Drilling Generated Heat on Damage Factor in GFRP. *Key Engineering Materials* 594–595 (December 2013): 661–665. DOI: 10.4028/www.scientific.net/kem.594-595.661

24. David-Müzel S, Bonhin EP, Ribeiro MV, et al. Furfuryl resin/CNT/carbon fiber drilling, using carbide drill coated with Balinit-Helica. *Mater Manuf Process* 2020; 35: 1096–1103. DOI: 10.1080/10426914.2020.1765252.

25. Erturk AT, Vatansever F, Yarar E, et al. Effects of cutting temperature and process optimization in drilling of GFRP composites. *J Compos Mater* 2020; 15. Article; Early Access. DOI: 10.1177/0021998320947143.

26. Liu LP, Qi CL, Wu F, et al. Analysis of thrust force and delamination in drilling GFRP composites with candle stick drills. *Int J Adv Manuf Tech* 2018; 95: 2585–2600. Article. DOI: 10.1007/s00170-017-1369-8.

27. Kar KK. *Composite Materials: Processing, Applications, Characterizations*. Berlin, Heidelberg: Springer, 2016.

28. Sheikh-Ahmad JY. *Machining of Polymer Composites*. New York, NY: Springer, 2009.

29. Singh I, Bhatnagar N and Viswanath P. Drilling of uni-directional glass fiber reinforced plastics: Experimental and finite element study. *Mater Des* 2008; 29: 546–553. DOI: 10.1016/j.matdes.2007.01.029.

30. Krishnamoorthy A, Boopathy SR and Palanikumar K. Delamination analysis in drilling of CFRP composites using response surface methodology. *J Compos Mater* 2009; 43: 2885–2902. DOI: 10.1177/0021998309345309.

31. Rawat S and Attia H. Characterization of the dry high speed drilling process of woven composites using Machinability Maps approach. *CIRP Ann* 2009; 58: 105–108. DOI: 10.1016/j.cirp.2009.03.100.

32. Agirregomezkorta A, Sánchez-Soto M, Aretxaga G, et al. Effects of vacuum infusion processing parameters on the impact behavior of carbon fiber reinforced cyclic butylene terephthalate composites. *J Compos Mater* 2014; 48: 333–344.

33. Campos Rubio J, Panzera TH, Abrao AM, et al. Effects of high speed in the drilling of glass whisker-reinforced polyamide composites (PA66 GF30): statistical analysis of the roughness parameters. *J Compos Mater* 2011; 45: 1395–1402. DOI: 10.1177/0021998310381540.

34. Sonkar V, Abhishek K, Datta S, et al. Multi-objective optimization in drilling of GFRP composites: a degree of similarity approach. *Proced Mater Sci* 2014; 6: 538–543. DOI: 10.1016/j.mspro.2014.07.068.

35. Palanikumar K. Experimental investigation and optimisation in drilling of GFRP composites. *Measurement* 2011; 44: 2138–2148. DOI: 10.1016/j.measurement.2011.07.023.

36. sunny T, Babu J and Philip J. Experimental studies on effect of process parameters on delamination in drilling GFRP composites using taguchi method. *Proced Mater Sci* 2014; 6: 1131–1142. DOI: 10.1016/j.mspro.2014.07.185.

37. Hansda S and Banerjee S. Optimizing multi characteristics in drilling of GFRP composite using utility concept with taguchi's approach. *Proced Mater Sci* 2014; 6: 1476–1488. DOI: 10.1016/j.mspro.2014.07.127.

38. Khashaba UA. Drilling of polymer matrix composites: a review. *J Compos Mater* 2012; 47: 1817–1832. DOI: 10.1177/0021998312451609.

39. Malik K, Ahmad F and Gunister E. Drilling performance of natural fiber reinforced polymer composites: a review. *J Nat Fibers* 2021: 1–19. DOI: 10.1080/15440478.2020.1870624.

40. Geier N, Davim JP and Szalay T. Advanced cutting tools and technologies for drilling carbon fibre reinforced polymer (CFRP) composites: a review. *Composites A: Appl Sci Manufacturing* 2019; 125: 105552. DOI: 10.1016/j.compositesa.2019.105552.

41. Khashaba UA, El-Sonbaty IA, Selmy AI, et al. Machinability analysis in drilling woven GFR/epoxy composites: Part I – Effect of machining parameters. *Composites Part A: Appl Sci Manufacturing* 2010; 41: 391–400. DOI: 10.1016/j.compositesa.2009.11.006.

42. Campos Rubio J, Abrao AM, Faria PE, et al. Effects of high speed in the drilling of glass fibre reinforced plastic: evaluation of the delamination factor. *Int J Machine Tools Manufacture* 2008; 48: 715–720. DOI: 10.1016/j.ijmachtools.2007.10.015.

43. Kishore R, Tiwari R and Singh I. Investigation of drilling in [(0/90)/0] s glass fibre reinforced plastics using taguchi method. *J Adv Prod Eng Manangement* 2009; 4: 37–46.

44. Tsao CC and Chiu YC. Evaluation of drilling parameters on thrust force in drilling carbon fiber reinforced plastic (CFRP) composite laminates using compound core-special drills. *Int J Machine Tools Manufacture* 2011; 51: 740–744, DOI: 10.1016/j.ijmachtools.2011.05.004.

45. Tsao CC and Hocheng H. Evaluation of thrust force and surface roughness in drilling composite material using Taguchi analysis and neural network. *J Mater Process Tech* 2008; 203: 342–348, DOI: 10.1016/j.jmatprotec.2006.04.126.

46. Palanikumar K and Davim JP. Assessment of some factors influencing tool wear on the machining of glass fibre-reinforced plastics by coated cemented carbide tools. *J Mater Process Tech* 2009; 209: 511–519, DOI: 10.1016/j.jmatprotec.2008.02.020.

47. Murthy B, Rodrigues L and Devineni A. Process parameters optimization in GFRP drilling through integration of Taguchi and response surface methodology. *J Res J Recent Sci* 2012; 2277: 2502.

48. Vasudevan H, Rajguru RR and Deshpande NC. Multiobjective optimization of drilling characteristics for NEMA G-11 GFRP/Epoxy composite using desirability coupled with taguchi method. *Proced Eng* 2014; 97: 522–530.

49. Murthy B, Rodrigues LR, Sharma NY, et al. Influence of process parameters on the quality of hole in drilling of GFRP composites-an experimental investigation using DOE. In: International Conference on Mechanical and Electrical Technology 2010, 10–12 September 2010. IEEE, 2010, pp. 87–90.

50. Liu D, Chen W and Chen Z. Study of thrust force and torque in drilling carbon fibre reinforced plastics(CFRP) using twist drill brazed diamond. In: 2nd International Asia Conference on Informatics in Control, Automation and Robotics CAR 2010, 6–7 March 2010, pp. 44–47.

51. Abrao A, Rubio JC, Faria P, et al. The effect of cutting tool geometry on thrust force and delamination when drilling glass fibre reinforced plastic composite. *Mater Des* 2008; 29: 508–513.

52. Altin Karataş M and Gökkaya H. A review on machinability of carbon fiber reinforced polymer (CFRP) and glass fiber reinforced polymer (GFRP) composite materials. *Defence Tech* 2018; 14: 318–326, DOI: 10.1016/j.dt.2018.02.001.

53. Faria P, Campos R, Abrao A, et al. Thrust force and wear assessment when drilling glass fiber-reinforced polymeric composite. *J Compos Mater* 2008; 42: 1401–1414.

54. Pantawane P and Ahuja B. Experimental investigations and multi-objective optimization of friction drilling process on AISI 1015. *Int Journal Applied Engineering Research* 2011; 2: 448–461.

55. Balzers OO. BALINIT® HELICA: Gives Your Drills that Extra Twis, https://www.oerlikon.com/ecomaXL/files/oerlikon_HQ002EN (accessed 14 01 2022).

56. David-Müzel S, Bonhin EP, Ribeiro MV, et al. Furfuryl resin/CNT/carbon fiber drilling, using carbide drill coated with Balinit-Helica. *Mater Manufacturing Process* 2020: 1–8. DOI: 10.1080/10426914.2020.1765252.

57. Stephenson DA and Agapiou JS. *Metal Cutting Theory and Practice*. CRC Press, 2016.

58. Weinert K and Kempmann C. Cutting temperatures and their effects on the machining behaviour in drilling reinforced. *Plast Composites* 2004; 6: 684–689, DOI: 10.1002/adem.200400025.

59. Jayabal S and Natarajan U. Drilling analysis of coir-fibre-reinforced polyester composites. *Bull Mater Sci* 2011; 34: 1563–1567. DOI: 10.1007/s12034-011-0359-y.

60. Kalss W, Reiter A, Derflinger V, et al. Modern coatings in high performance cutting applications. *Int J Refractory Met Hard Mater* 2006; 24: 399–404.